Hindawi Publishing Corporation
Mathematical Problems in Engineering
Volume 2009, Article ID 384071, 16 pages
doi:10.1155/2009/384071

Research Article

The Determination of the Velocities after Impact for the Constrained Bar Problem

André Fenili,[1] Luiz Carlos Gadelha de Souza,[2] and Bernd Schäfer[3]

[1] *Center for Engineering, Modeling and Applied Social Sciences (CECS), Federal University of ABC (UFABC), Aerospace Engineering, Av. dos Estados, 5001. Bloco B/Sala 936, 09210-580 Santo André, SP, Brazil*
[2] *National Institute for Space Research—INPE, Av. dos Astronautas, 1758, 12201-940 São José dos Campos, SP, Brazil*
[3] *German Aerospace Center—DLR, Institute of Robotics and Mechatronics, 82234 Wessling, Germany*

Correspondence should be addressed to Luiz Carlos Gadelha de Souza, gadelha@dem.inpe.br

Received 27 May 2009; Accepted 23 November 2009

Recommended by Antonio Prado

A simple mathematical model for a constrained robotic manipulator is investigated. Besides the fact that this model is relatively simple, all the features present in more complex problems are similar to the ones analyzed here. The fully plastic impact is considered in this paper. Expressions for the velocities of the colliding bodies after impact are developed. These expressions are important in the numerical integration of the governing equations of motion when one must exchange the set of unconstrained equations for the set of constrained equation. The theory presented in this work can be applied to problems in which robots have to follow some prescribed patterns or trajectories when in contact with the environment. It can also de applied to problems in which robotic manipulators must handle payloads.

1. Introduction

There are several ways to deal with the problem of interaction between bodies. Impact dynamics and continuous contact between bodies can both be included in the mathematical model of the constrained problem, or just one of these effects can be considered. It depends, obviously, on the characteristics of the studied problem.

The investigations about the contact between bodies include (at least) two different kind of analysis [1]: one associated with the beginning of contact and one associated with its termination. In the first analysis, the distance between the bodies must be checked in order to know when contact occurs; in the second analysis, once the contact is established, the reaction

(normal; compression) force between the bodies must be checked. In the second analysis, contact finishes when the contact force is equal to zero.

One of the hardest parts in the study of contact problems involves the different models that must be developed for contact and noncontact situations and the switching between these models when integrating the equations of motion [2, 3]. The unconstrained problem and the constrained problem do not have the same number of degrees of freedom. Dynamic systems when constrained have less degrees of freedom than when unconstrained.

The transition between constrained and unconstrained motions is sometimes called contact (including impact) and sometimes called just impact (mostly when the bodies separate after the collision). When contact occurs, the new velocities of the bodies involved must be known in order to generate the initial conditions to the second part (constrained problem) of the numerical integration. In the constrained problem, the concept of coefficient of restitution is very important [4].

2. Geometric Model of the System and Governing Equations of Motion

The problem discussed here is depicted in Figure 1. According to this figure, in a part of its trajectory, the free end of the bar moves along the constraint represented by the mass named m_w. All the movements occur in the horizontal plane. When contact occurs, impact and bouncing are also allowed to occur.

The mass in which the rigid bar is pivoted (m_s) oscillates when excited by the movement of the bar (free and constrained). In the axis Z, passing through the connection between the bar and m_s (perpendicular to the paper sheet), there is a prescribed moment, M_θ, acting to turn the bar.

The dashed lines represent the position of the masses in which the springs and dampers are free of forces. The dotted line represents the position from which one starts to count the angular displacement, θ.

In physical terms, this system may represent a robot with a translational joint and a rotational joint; m_w can be thought as an obstructing wall on the robot's trajectory (or some object this robot must handle or interact with), and M_θ can be thought as an external torque provided by a dc motor.

According to [5], the constrained governing equations of motion for this system are given by

$$\begin{aligned}
&(m_b + m_s)\ddot{y}_s + c_s\dot{y}_s + k_s y_s - m_b\ d_{Acmb}\dot{\theta}^2 \sin\theta + m_b d_{Acmb}\ddot{\theta}\cos\theta + F_N = 0,\\
&m_w\ddot{y}_w + c_w\dot{y}_w + k_w y_w - F_N = 0,\\
&\left(I_{b,\mathrm{cm}} + m_b d_{Acmb}^2\right)\ddot{\theta} + m_b d_{Acmb}\ddot{y}_s\cos\theta + F_N\ell\cos\theta = M_\theta,
\end{aligned} \tag{2.1}$$

and the constraint condition is given by

$$d - y_s + y_w - \ell\sin\theta = 0, \tag{2.2}$$

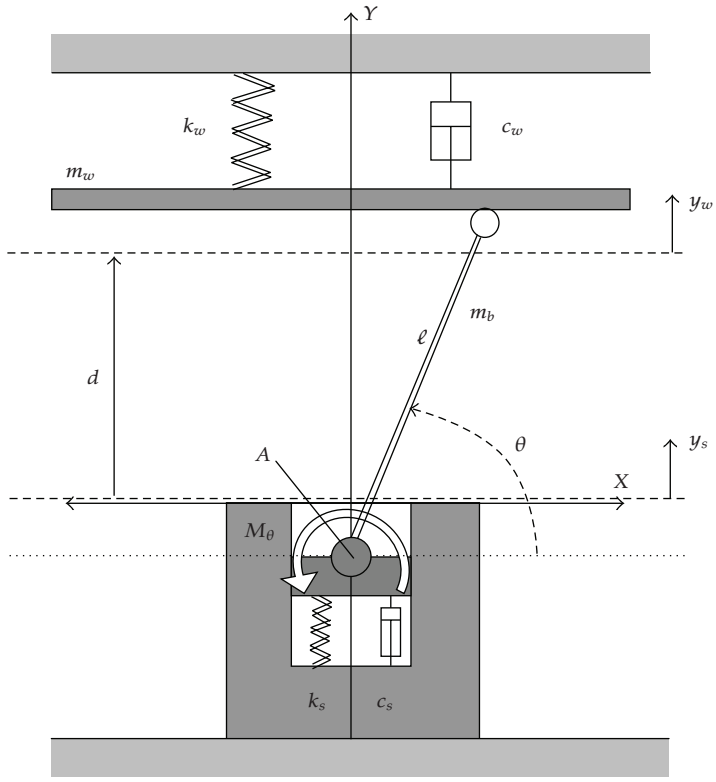

Figure 1: Oscillating constrained bar.

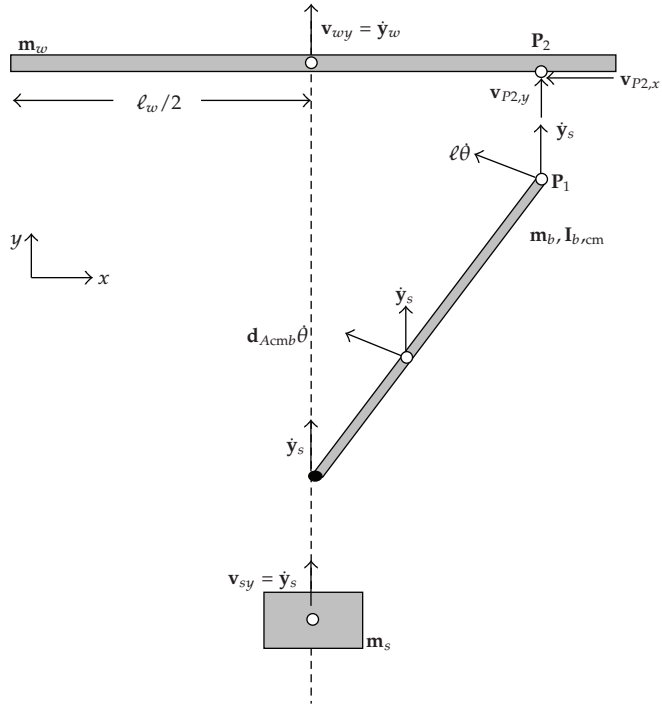

Figure 2: Velocities.

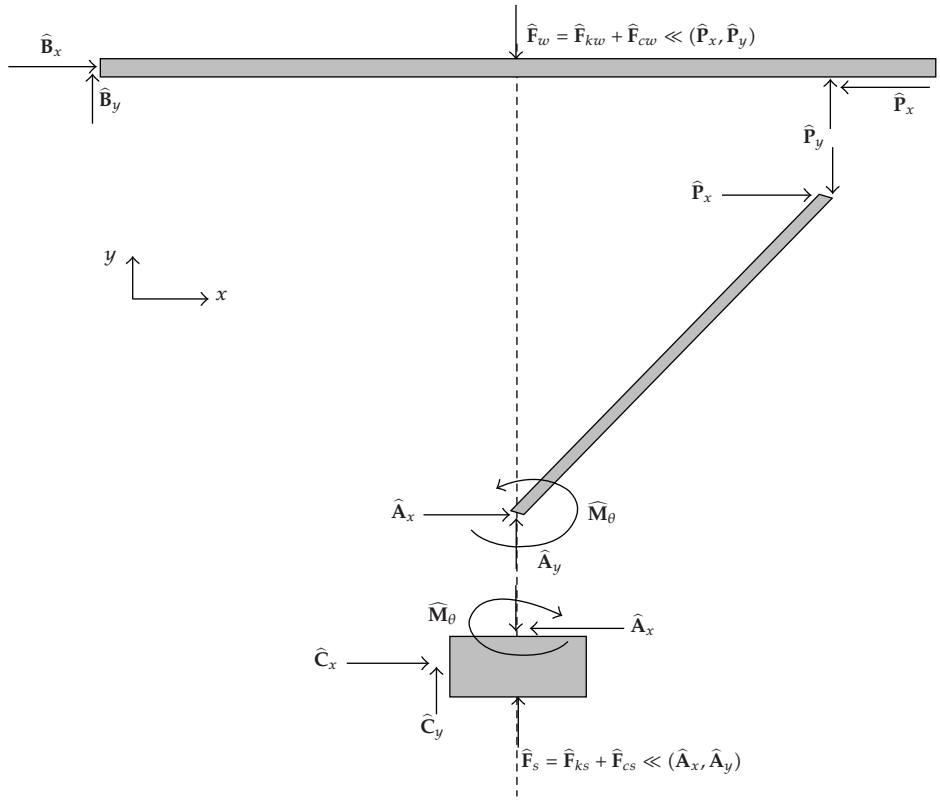

Figure 3: Impulses.

where $I_{b,\mathrm{cm}}$ represents the bar moment of inertia around its center of mass, m_b represents the mass of the bar, d_{Acmb} represents the distance from A to the cm of the bar, c_w represents the damping coefficient of m_w, c_s represents the damping coefficient associated with mass m_s, k_w represents the stiffness coefficient of mass m_w, k_s represents the stiffness coefficient associated with m_s, and F_N represents the amplitude of the normal force. It is assumed the there are no friction forces involved and ℓ represents the total length of the bar.

Equations (2.1) are the equations of motion for y_s, y_w, and θ. Equation (2.2) is an additional relationship between the generalized coordinates y_s, θ and y_w when contact occurs. Equations from (2.1) to (2.2) provide four equations and four unknowns (y_s, θ, y_w, and F_N) considering the constrained problem and three equations and three unknowns (y_s, θ, and y_w) considering the unconstrained problem. In the unconstrained case, (2.2) does not apply and $F_N = 0$.

3. The Contact Case

In contact, for this problem, there is the loss of one degree of freedom. In other words, one of the variables is dependent on all the others. The best choice is the elimination of the generalized coordinate y_w, which is not always present into the system represented by the

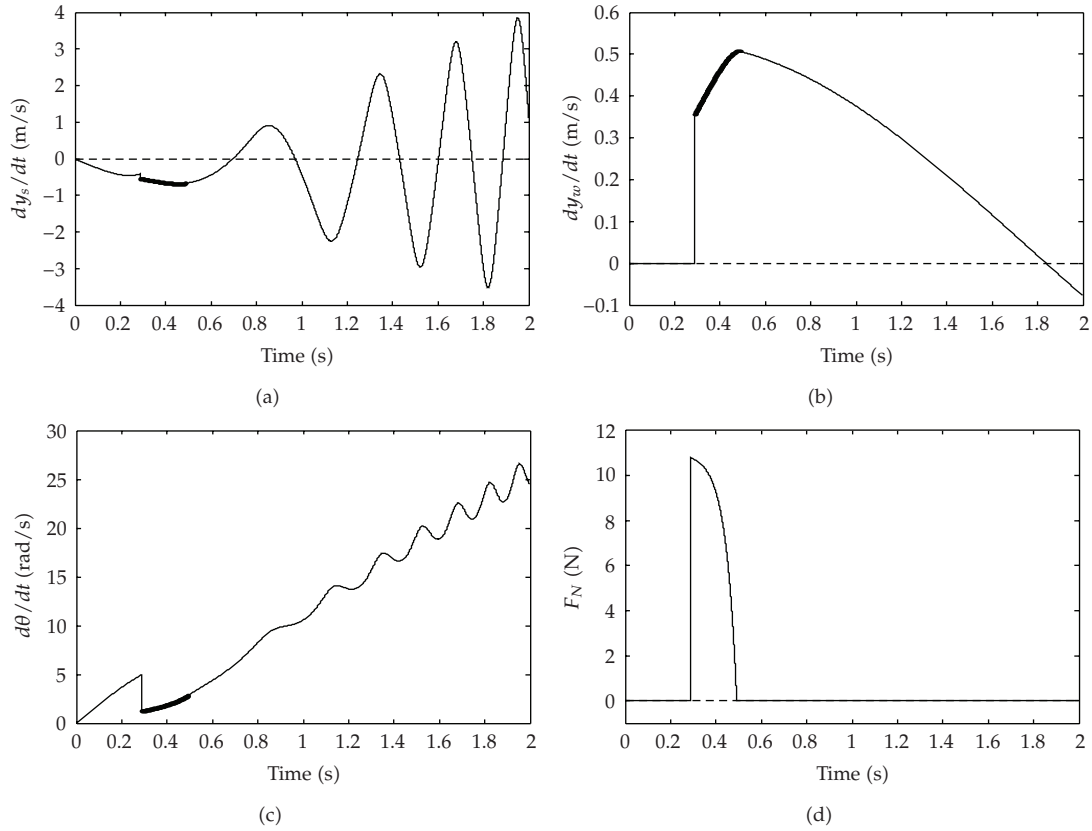

Figure 4: $\dot{y}_s$, $\dot{y}_w$, $\dot{\theta}$, and F_N considering $k_w = 10\,\text{Nm}$.

oscillating bar [6]. The new set of equations [5] is given by

$$\begin{aligned}
&\ddot{y}_s + \frac{1}{a_1 m_t + a_3 \cos^2\theta}\big(a_1(c_s + c_w)\dot{y}_s + a_1(k_s + k_w)y_s + a_1 c_w \ell\dot{\theta}\cos\theta + a_1 k_w \ell \sin\theta - a_1 a_2 \dot{\theta}^2 \sin\theta \\
&\quad - m_b c_w \ell^2 d_{Acmb}\dot{\theta}\cos^3\theta - m_b k_w \ell^2 d_{Acmb}\sin\theta\cos^2\theta \\
&\quad + m_b k_w d\ell d_{Acmb}\cos^2\theta + \ell(m_w \ell c_s - m_b d_{Acmb} c_w)\dot{y}_s\cos^2\theta \\
&\quad + \ell(m_w \ell k_s - m_b d_{Acmb} k_w)y_s\cos^2\theta - a_1 k_w d\big) = -\frac{a_2\cos\theta}{a_1 m_t + a_3\cos^2\theta}M_\theta, \\
&\ddot{\theta} + \frac{1}{a_1 m_t + a_3\cos^2\theta}\big(c_w\ell(m_t\ell - a_2)\dot{\theta}\cos^2\theta + k_w\ell(m_t\ell - a_2)\sin\theta\cos\theta - k_w d(m_t\ell - a_2)\cos\theta \\
&\quad + (a_2 m_b d_{Acmb} - m_w\ell(m_t\ell - a_2))\dot{\theta}^2\sin\theta\cos\theta + (k_w(m_t\ell - a_2) - a_2 k_s)y_s\cos\theta \\
&\quad + (c_w(m_t\ell - a_2) - a_2 c_s)\dot{y}_s\cos\theta\big) = \frac{m_t}{a_1 m_t + a_3\cos^2\theta}M_\theta.
\end{aligned} \tag{3.1}$$

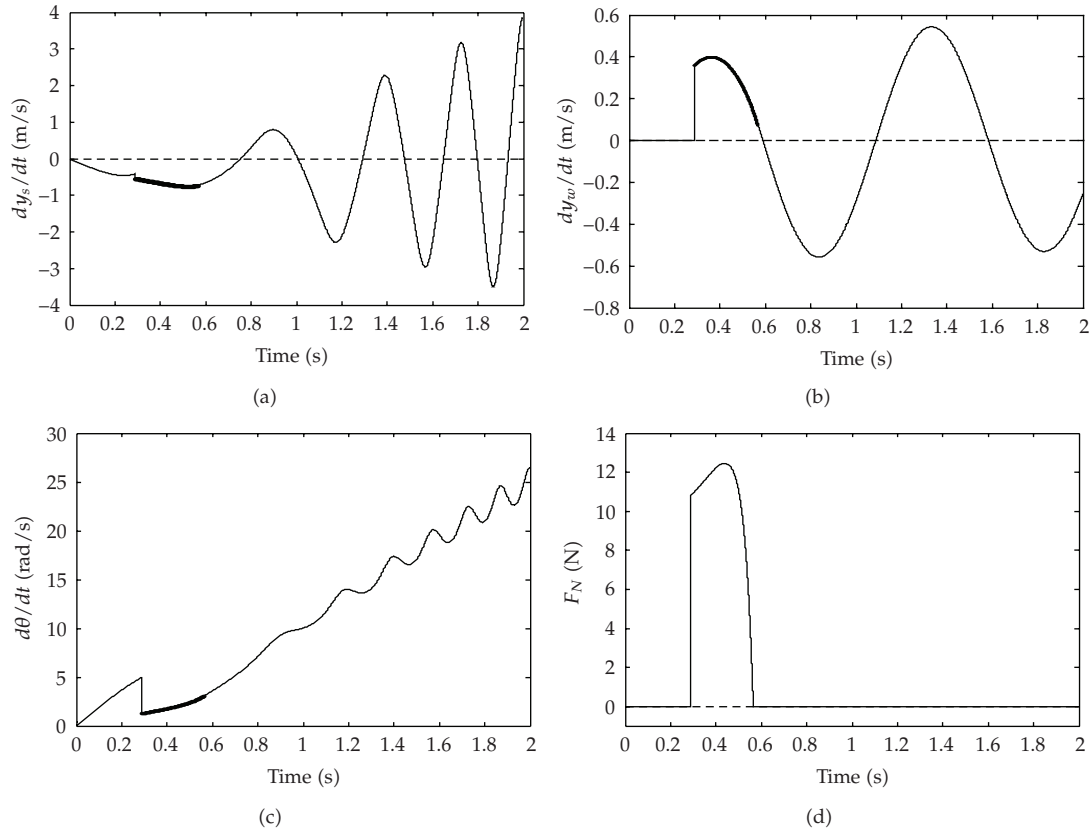

Figure 5: $\dot{y}_s$, $\dot{y}_w$, $\dot{\theta}$, and F_N considering $k_w = 400\,\text{Nm}$.

The fully plastic impact case is considered here for the calculation of the velocities immediately after contact. Separation will take place when the normal force is zero.

As soon as these two variables are known, the remaining variable, y_w, is also known through (2.2). Equations (3.1) represent, respectively, the time behavior of the generalized coordinates y_s and θ during the contact condition. In [5], an analytical expression to the reaction force, F_N, is also presented.

4. The Determination of the Velocities after Contact (Impact)

The equations for the impact are formulated for point P (see Figure 2 for the representation of the velocities of the three bodies) where, for sake of clarity, it is distinguished between Point P_1 belonging to the wall and point P_2 belonging to the bar. Figure 3 shows the free body diagram for the three rigid bodies indicating not the forces at the points of connection or contact but rather indicating the equivalent linear impulses due to impact. All these quantities are marked with an overhead symbol "hat", for example, $\widehat{P}_x$, which is the linear impulse of the equivalent force P_x. The physical dimension is the same as the linear momentum, that is, $N \cdot s$, except for the angular impulse $\widehat{M}_\theta$ whose unit is Nm · s.

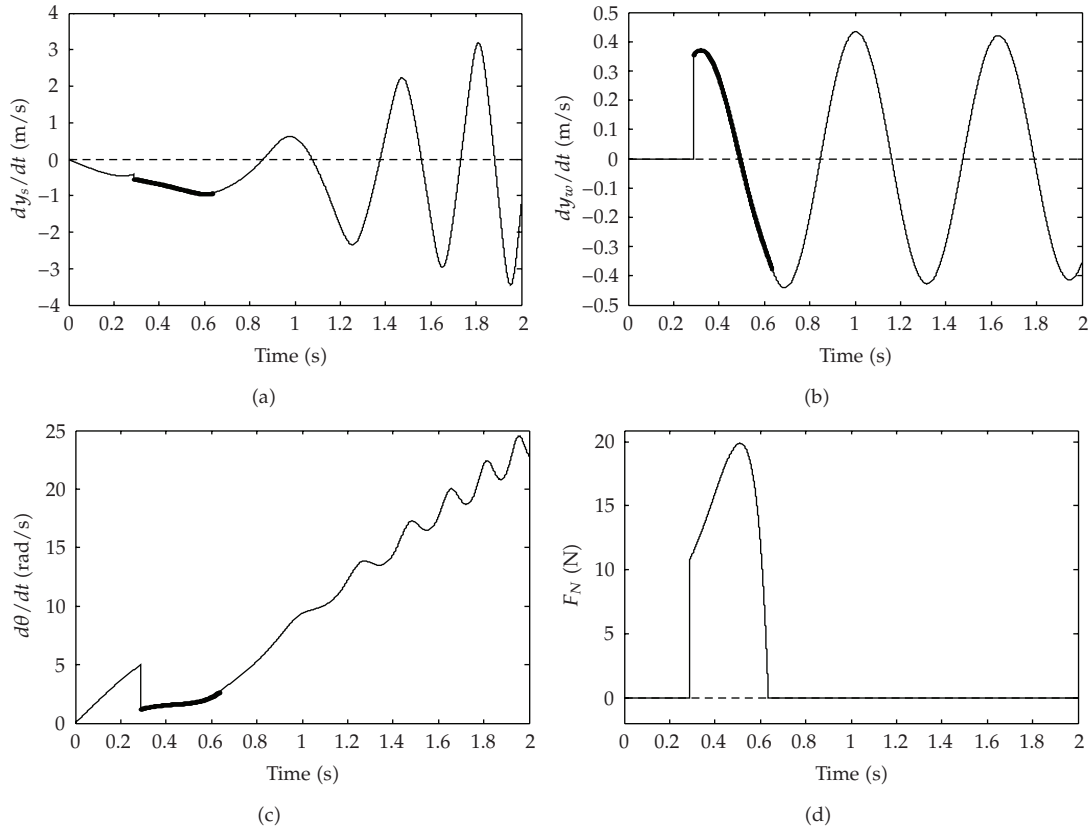

Figure 6: $\dot{y}_s$, $\dot{y}_w$, $\dot{\theta}$, and F_N considering $k_w = 1000\,\text{Nm}$.

For each of the three rigid bodies, we can formulate now the linear impulse/linear momentum equations in the two directions x and y. Additionally, for the rotating bodie(s), we have the equivalent angular impulse/angular momentum equation in z-direction, formulated w.r.t. to the respective centre of mass.

To better distinguish between velocities right before and right after impact, they are denoted with superscripts "+" (after) and "−" (before). Their two components in x- and y-directions are indicated by corresponding subscripts "x" and "y".

And, to be more general, it is also allowed initially for the rigid bodies with masses m_s and m_w to rotate as well. The respective angular velocities therefore will be denoted by ω with appropriate indices. Later, this additional degree of freedom will be kinematically constrained.

For the wall, it is obtained that

$$\begin{aligned} m_w v_{wy}^{+} - m_w v_{wy}^{-} &= \widehat{P}_y - \widehat{F}_w, \\ m_w v_{wx}^{+} - m_w v_{wx}^{-} &= -\widehat{P}_x + \widehat{B}_x, \\ I_w \omega_w^{+} - I_w \omega_w^{-} &= -\widehat{B}_y \frac{\ell_w}{2} + \widehat{P}_y \ell \sin\theta. \end{aligned} \tag{4.1}$$

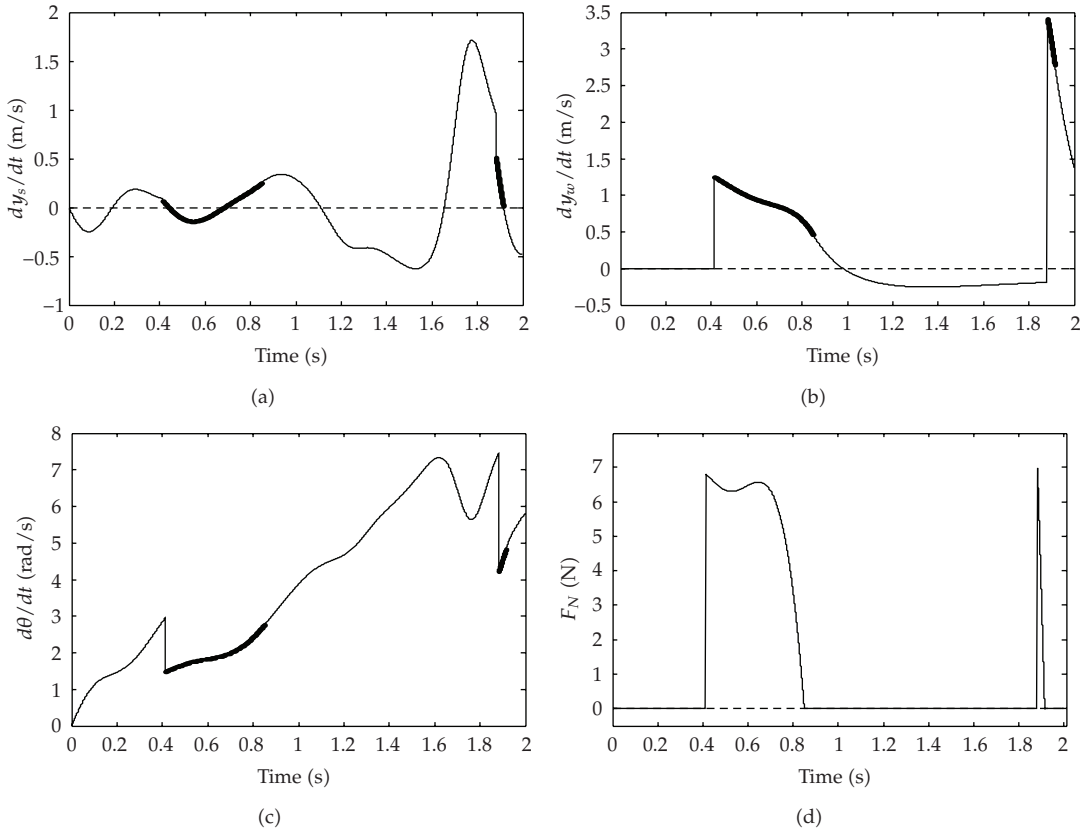

Figure 7: $\dot{y}_s$, $\dot{y}_w$, $\dot{\theta}$, and F_N considering $M_\theta = 5\text{Nm}$.

For the bar, it is obtained ($\omega_b \equiv \dot{\theta}$) that

$$\begin{aligned} m_b v_{by}^+ - m_b v_{by}^- &= \widehat{A}_y - \widehat{P}_y, \\ m_b v_{bx}^+ - m_b v_{bx}^- &= \widehat{A}_x + \widehat{P}_x, \\ I_{b,\mathrm{cm}}\omega_b^+ - I_{b,\mathrm{cm}}\omega_b^- &= \widehat{M}_\theta + \widehat{A}_x d_{Acmb}\sin\theta - \widehat{A}_y d_{Acmb}\cos\theta \\ &\quad - \widehat{P}_x(\ell - d_{Acmb})\sin\theta - \widehat{P}_y(\ell - d_{Acmb})\cos\theta. \end{aligned} \tag{4.2}$$

And, finally, for the lower rigid body with mass m_s, it is obtained that

$$\begin{aligned} m_s v_{sy}^+ - m_s v_{sy}^- &= -\widehat{A}_y + \widehat{C}_y + \widehat{F}_s, \\ m_s v_{sx}^+ - m_s v_{sx}^- &= -\widehat{A}_x + \widehat{C}_x, \\ I_s\omega_s^+ - I_s\omega_s^- &= -\widehat{M}_\theta + \widehat{A}_x b_{sy} - \widehat{C}_y b_{sx}, \end{aligned} \tag{4.3}$$

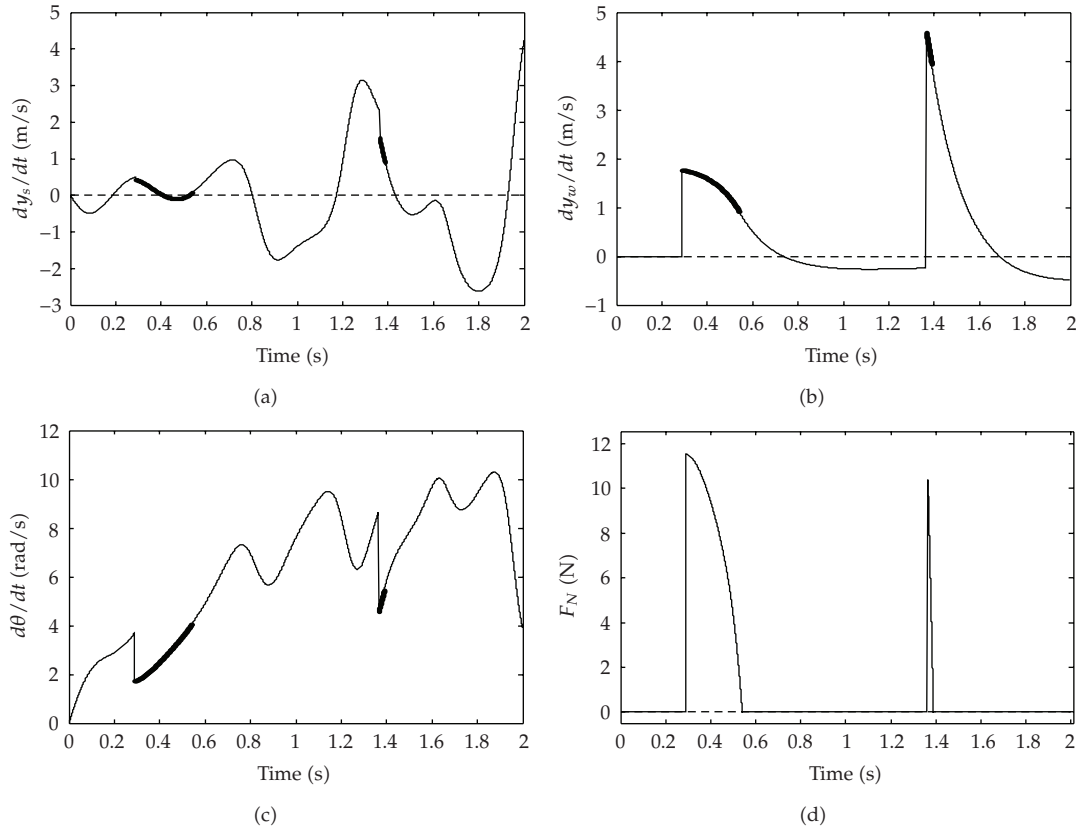

Figure 8: $\dot{y}_s$, $\dot{y}_w$, $\dot{\theta}$, and F_N considering $M_\theta = 10\,\text{Nm}$.

assuming that the directions of $\widehat{C}_x$ and $\widehat{F}_s$ are going through the center of mass. The geometric quantities b_{sx} and b_{sy}, not shown in Figure 3, denote the distances of the respective linear impulses measured from the center of mass.

These equations simplified if the following assumptions are made.

(1) The external two linear impulses $\widehat{F}_w$ and $\widehat{F}_s$, and the angular impulse $\widehat{M}_\theta$ are small compared with the internal impulses; therefore, they can be neglected.

(2) The rotational motion of both, the wall and the lower rigid body, is omitted; therefore, one has $\omega_w = 0$ and $\omega_s = 0$.

(3) The wall is allowed to move only in the vertical direction, as well as the lower rigid body; therefore, $v_{wx} = 0$ and $v_{sx} = 0$.

(4) The contact surface between the lower rigid body and the left or right vertical guiding surface (not shown in the figures) is assumed ideally smooth; therefore, $\widehat{C}_y = 0$.

(5) The contact zone between the free end of the bar and the wall surface is also assumed ideally smooth; therefore, $\widehat{P}_x = 0$. Otherwise, if this surface is rough, we have to account for an additional velocity relationship, for example, given by the definition of the coefficient of restitution in x-direction.

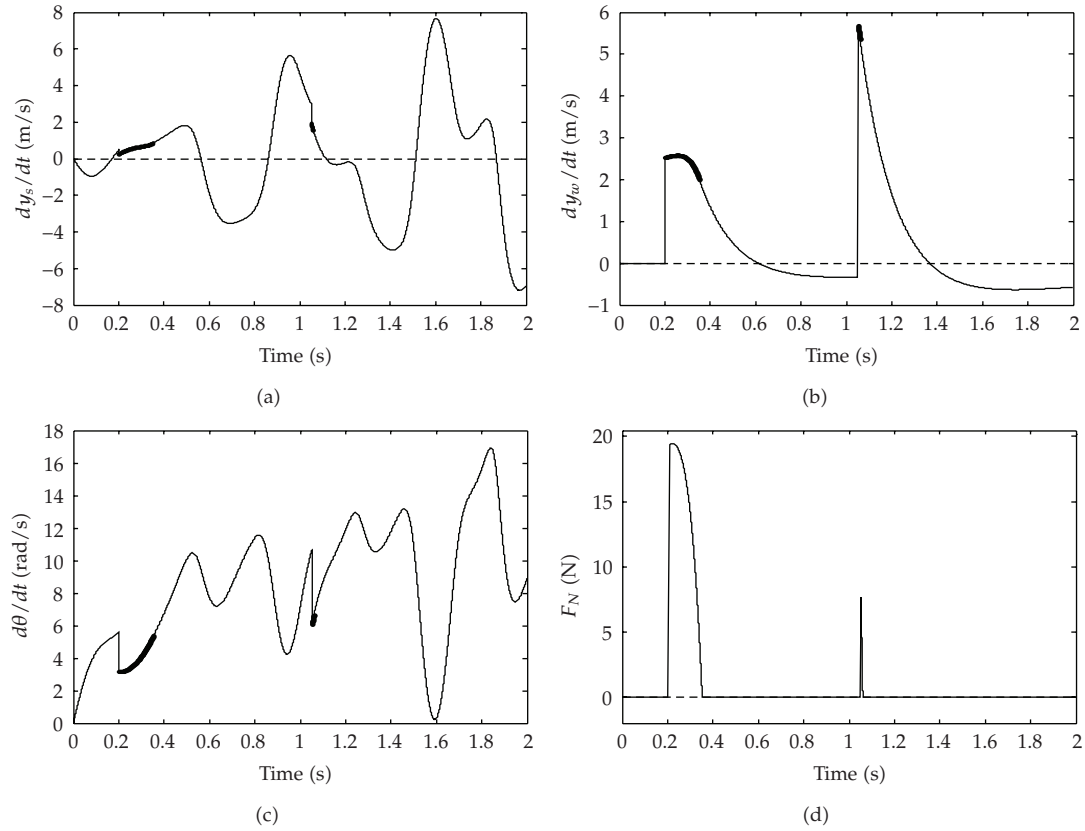

Figure 9: $\dot{y}_s$, $\dot{y}_w$, $\dot{\theta}$, and F_N considering $M_\theta = 20\,\text{Nm}$.

Applying these assumptions, the following set of equations is obtained:

$$m_w v_{wy}^{+} - m_w v_{wy}^{-} = \widehat{P}_y, \tag{4.4}$$

$$\widehat{B}_x = \widehat{P}_x = 0, \tag{4.5}$$

$$\widehat{B}_y = \frac{2\ell}{\ell_w} \sin\theta \cdot \widehat{P}_y \ , \tag{4.6}$$

$$m_b v_{by}^{+} - m_b v_{by}^{-} = \widehat{A}_y - \widehat{P}_y, \tag{4.7}$$

$$m_b v_{bx}^{+} - m_b v_{bx}^{-} = \widehat{A}_x + \widehat{P}_x = \widehat{A}_x, \tag{4.8}$$

$$I_{b,\text{cm}}\omega_b^{+} - I_{b,\text{cm}}\omega_b^{-} = \widehat{A}_x d_{Acmb} \sin\theta - \widehat{A}_y d_{Acmb} \cos\ \theta - \widehat{P}_y(\ell - d_{Acmb}) \cos\ \theta, \tag{4.9}$$

$$m_s v_{sy}^{+} - m_s v_{sy}^{-} = -\widehat{A}_y \ , \tag{4.10}$$

$$\widehat{C}_x = \widehat{A}_x, \tag{4.11}$$

$$b_{sy} = 0. \tag{4.12}$$

In order to calculate the velocities at the point of impact, P, only (4.4) and (4.7) to (4.10) are of interest. Additionally, it is needed to establish some kinematic relationships. For the bar center of mass, one has

$$\begin{aligned}\mathbf{v}_b &= \mathbf{v}_s + \boldsymbol{\omega}_b \times \mathbf{r}_{ASb} \\ &= \left(-\omega_b d_{Acmb} \sin\theta, v_{sy} + \omega_b d_{Acmb} \cos\ \theta\right)^T \\ &= \left(v_{bx}, v_{by}\right)^T,\end{aligned} \tag{4.13}$$

where the length of the vector $\mathbf{r}_{Acmb}$ is just $|\mathbf{r}_{Acmb}| = d_{Acmb}$. Equation (4.13) is valid for the velocity right before and after impact. For the free end of the bar, it is obtained equivalently

$$\begin{aligned}\mathbf{v}_{P1} &= \mathbf{v}_s + \boldsymbol{\omega}_b \times \mathbf{r}_{AP1} \\ &= \left(-\omega_b \ell \sin\theta, v_{sy} + \omega_b \ell \cos\theta\right)^T \\ &= \left(v_{P1x}, v_{P1y}\right)^T\end{aligned} \tag{4.14}$$

with $|\mathbf{r}_{AP1}| = \ell$. In the same way as (4.13), equation (4.14) is valid for the velocity right before impact and right after. During impact, one has the additional equation, which relates the velocities before and after impact at point P, in the direction normal to the contact surface, that is, in y-direction:

$$\varepsilon_y = -\frac{v_{P1y}^+ - v_{P2y}^+}{v_{P1y}^- - v_{P2y}^-} \tag{4.15}$$

with

$$\begin{aligned}v_{P1y}^- &= v_{sy}^- + \omega_b^- \ell \cos\theta, \\ v_{P1y}^+ &= v_{sy}^+ + \omega_b^+ \ell \cos\theta, \\ v_{P2y}^- &= v_{wy}^- = y_w^-, \\ v_{P2y}^+ &= v_{wy}^+ = y_w^+.\end{aligned} \tag{4.16}$$

In the following, it is assumed that there is a fully plastic impact, that is, the impacting bodies maintain steady contact as far as the contact force is repulsive (otherwise, they will separate). This leaves $\varepsilon_y = 0$, and hence

$$v_{P1y}^+ = v_{P2y}^+ \tag{4.17}$$

or

$$v_{wy}^+ = v_{sy}^+ + \omega_b^+ \ell \cos\theta = v_{by}^+ + \omega_b^+ (\ell - d_{Acmb}) \cos\theta. \tag{4.18}$$

With these equations, it is possible to calculate all the velocities right after impact, given the velocities before impact. Additionally, but not needed here, it is also possible to calculate the appropriate linear impulses. To summarize, one has the following eight equations to determine all the five velocities right after impact $(v_{sy}^{+}, v_{bx}^{+}, v_{by}^{+}, v_{wy}^{+}, \omega_b^{+})$, as well as the impulses $(\widehat{A}_x, \widehat{A}_y, \widehat{P}_y)$:

$$m_w v_{wy}^{+} - m_w v_{wy}^{-} = \widehat{P}_y, \tag{4.19}$$

$$m_b v_{by}^{+} - m_b v_{by}^{-} = \widehat{A}_y - \widehat{P}_y, \tag{4.20}$$

$$m_b v_{bx}^{+} - m_b v_{bx}^{-} = \widehat{A}_x, \tag{4.21}$$

$$I_{b,\mathrm{cm}}\omega_b^{+} - I_{b,\mathrm{cm}}\omega_b^{-} = \widehat{A}_x d_{Acmb}\sin\theta - \widehat{A}_y d_{Acmb}\cos\theta - \widehat{P}_y(\ell - d_{Acmb})\cos\theta, \tag{4.22}$$

$$m_s v_{sy}^{+} - m_s v_{sy}^{-} = -\widehat{A}_y, \tag{4.23}$$

$$v_{bx}^{+} = -\omega_b^{+} d_{Acmb}\sin\theta, \tag{4.24}$$

$$v_{by}^{+} = v_{sy}^{+} + \omega_b^{+} d_{Acmb}\cos\theta, \tag{4.25}$$

$$v_{wy}^{+} = v_{sy}^{+} + \omega_b^{+}\ell\cos\theta = v_{by}^{+} + \omega_b^{+}(\ell - d_{Acmb})\cos\theta. \tag{4.26}$$

Initially, all the impulses are obtained. $\widehat{A}_y$ is simply obtained from (4.23) or by adding the two (4.19) and (4.20), giving

$$\widehat{A}_y = -\left(m_s v_{sy}^{+} - m_s v_{sy}^{-}\right) = m_b v_{by}^{+} - m_b v_{by}^{-} + m_w v_{wy}^{+} - m_w v_{wy}^{-}. \tag{4.27}$$

$\widehat{A}_x$ also goes simply with (4.21),

$$\widehat{A}_x = m_b v_{bx}^{+} - m_b v_{bx}^{-} \tag{4.28}$$

and $\widehat{P}_y$ is simply obtained directly from (4.19) or by adding (4.20) and (4.23)

$$\widehat{P}_y = m_w v_{wy}^{+} - m_w v_{wy}^{-} = -\left(m_b v_{by}^{+} - m_b v_{by}^{-}\right) - \left(m_s v_{sy}^{+} - m_s v_{sy}^{-}\right). \tag{4.29}$$

Comparing (4.27) with (4.29), it is observed that both equations yield the same result for the linear momenta before and after impact. To determine now the velocities right after impact, one can rely on (4.22), (4.24), (4.25), (4.26), and (4.27) (or (4.29), which is the same).

Replacing v_{bx}^{+}, v_{by}^{+} and v_{wy}^{+}, one arrives at the two equations for the unknown velocities v_{sy}^{+} and ω_b^{+}:

$$\begin{aligned}
&(m_s + m_b + m_w)v_{sy}^{+} = m_s v_{sy}^{-} + m_b v_{by}^{-} + m_w v_{wy}^{-} - \omega_b^{+}(m_b d_{Acmb} + m_w \ell)\cos\theta,\\
&\left[I_{b,\mathrm{cm}} + m_b d_{Acmb}^2 \sin^2\theta + m_w \ell(\ell - d_{Acmb})\cos^2\theta\right]\omega_b^{+}\\
&\quad = v_{sy}^{+}[m_s d_{Acmb} - m_w(\ell - d_{Acmb})]\cos\theta + I_{b,\mathrm{cm}}\omega_b^{-} - m_s v_{sy}^{-} d_{Acmb}\cos\theta\\
&\quad - m_b v_{bx}^{-} d_{Acmb}\sin\theta + m_w v_{wy}^{-}(\ell - d_{Acmb})\cos\theta.
\end{aligned} \tag{4.30}$$

And with $v_{by}^{-} = v_{sy}^{-} + \omega_b^{-} d_{\mathrm{Acmb}}\cos\theta$, and $v_{bx}^{-} = -\omega_b^{-} d_{\mathrm{Acmb}}\sin\theta$, these equations can finally be expressed by means of the independent velocities, v_{sy}^{-}, v_{wy}^{-}, and ω_b^{-}, right before impact:

$$\begin{aligned}
&(m_s + m_b + m_w)v_{sy}^{+} = (m_s + m_b)v_{sy}^{-} + m_w v_{wy}^{-} + m_b \omega_b^{-} d_{Acmb}\cos\theta - \omega_b^{+}(m_b d_{Acmb} + m_w \ell)\cos\theta.\\
&\left[I_{b,\mathrm{cm}} + m_b d_{Acmb}^2 \sin^2\theta + m_w \ell(\ell - d_{Acmb})\cos^2\theta\right]\omega_b^{+}\\
&\quad = v_{sy}^{+}[m_s d_{Acmb} - m_w(\ell - d_{Acmb})]\cos\theta + \left(I_{b,\mathrm{cm}} + m_b d_{Acmb}^2 \sin^2\theta\right)\omega_b^{-}\\
&\quad - m_s v_{sy}^{-} d_{Acmb}\cos\theta + m_w v_{wy}^{-}(\ell - d_{Acmb})\cos\theta
\end{aligned} \tag{4.31}$$

With the abbreviations

$$\begin{aligned}
m_{\mathrm{tot}} &= m_s + m_b + m_w,\\
I_{\mathrm{tot}} &= I_{b,\mathrm{cm}} + m_b d_{Acmb}^2 \sin^2\theta + m_w \ell(\ell - d_{Acmb})\cos^2\theta,\\
r_1 &= (m_s + m_b)v_{sy}^{-} + m_w v_{wy}^{-} + m_b \omega_b^{-} d_{Acmb}\cos\theta,\\
r_2 &= -m_s v_{sy}^{-} d_{Acmb}\cos\theta + m_w v_{wy}^{-}(\ell - d_{Acmb})\cos\theta + \left(I_{b,\mathrm{cm}} + m_b d_{Acmb}^2 \sin^2\theta\right)\omega_b^{-},\\
\alpha_1 &= (m_b d_{Acmb} + m_w \ell)\cos\theta,\\
\alpha_2 &= [m_s d_{Acmb} - m_w(\ell - d_{Acmb})]\cos\theta,
\end{aligned} \tag{4.32}$$

one finally obtains

$$\begin{aligned}
v_{sy}^{+} &= \frac{r_1 I_{\mathrm{tot}} - r_2 \alpha_1}{\alpha_1 \alpha_2 + m_{\mathrm{tot}} I_{\mathrm{tot}}},\\
\omega_b^{+} &= \frac{r_1 \alpha_2 + r_2 m_{\mathrm{tot}}}{\alpha_1 \alpha_2 + m_{\mathrm{tot}} I_{\mathrm{tot}}}.
\end{aligned} \tag{4.33}$$

The denominator of these two equations then is written as

$$\begin{aligned}\alpha_1\alpha_2 + m_{\text{tot}}I_{\text{tot}} = {} & m_s m_b d_{Acmb}^2 + m_{\text{tot}}I_{b,\text{cm}} + m_b m_w\left[\ell(\ell - 2d_{Acmb})\cos^2\theta + d_{Acmb}^2\right] \\ & + m_s m_w \ell^2\cos^2\theta + m_b^2 d_{Acmb}^2\sin^2\theta.\end{aligned} \tag{4.34}$$

In order to check (4.33), one case is investigated; that is, for $\theta = 90°$, we should maintain the simple translational impact between the combined rigid body consisting of the two masses m_s and m_b and the wall with mass m_w. For the fully plastic impact, one then obtains from (4.33) with $\alpha_1 = 0$ and $\alpha_2 = 0$:

$$\begin{aligned}v_{sy}^{+}(\theta = 90°) &= \frac{r_1}{m_{\text{tot}}} = \frac{(m_s + m_b)v_{sy}^{-} + m_w v_{wy}^{-}}{m_{\text{tot}}}, \\ \omega_b^{+}(\theta = 90°) &= \frac{r_2}{I_{\text{tot}}} = \frac{I_{b,\text{cm}} + m_b d_{Acmb}^2}{I_{\text{tot}}}\omega_b^{-},\end{aligned} \tag{4.35}$$

where the first equation for the translational motion coincides with the result governed from simple impact of two rigid bodies.

5. Numerical Results

The values for the parameters used in the numerical simulations that follow are presented in Tables 1 and 2. The time step considered in the integration of the governing equations of motion is kept constant and equal to 0.0001 s. The fourth-order Runge-Kutta is the numerical integrator used. Two different classes of simulation are investigated.

The constant torque (with different amplitudes) was chosen because it is the simplest one, and in order to make the bar rotate always in the same direction and fulfill 360°. Any other kind of excitation (e.g., like a sinusoidal one with maximum amplitude of 180º, for instance) can be chosen without problem. In the simulation runs, the motion of the bar starts always in its horizontal position to the right, that is, with $\theta = 0°$.

The very beginning of contact is considered here as a fully plastic impact with impact time $\Delta t \approx 0$ and with $e = 0$, where e represents the coefficient of restitution. Contact finishes when $F_N = 0$. No friction or contact is considered, up to this point of the investigation, between m_s and the guide it slides through or between m_b and m_w.

5.1. Considering Different Values of k_w

When first contact takes place, m_w is at rest. The second contact (only shown here for the simulations varying M_θ) will happen with m_w presenting some velocity. The bar is able to develop many turns and, in fact, there are possibilities for it to reach many contact conditions as the time evolves.

According to Figures 4, 5, 6, 7, 8, and 9, the amplitude of F_N jumps at the beginning of contact, from zero (no contact) to a value associated with the impact force between the bodies. The contact force evolves with time according to the system states and properties. The value of F_N at the instant of impact does not necessarily represent the biggest value for

Table 1: Numerical values considered in the numerical simulations for different values of k_w.

Parameter	Value	Unity
m_b	2.00	Kg
m_s	5.00	Kg
m_w	10.00	Kg
k_s	5.00	Nm
	10.00	
k_w	400.00	Nm
	1000.00	
c_s	7.00	Ns/m
c_w	1.00	Ns/m
ℓ	1.00	m
d	0.60	m
d_{Acmb}	0.50	m
M_θ	10.00	Nm
$I_{b,\text{cm}}$	0.1667	Kg/m^2

Table 2: Numerical values considered in the numerical simulations for different values of M_θ.

Parameter	Value	Unity
m_b	2.00	Kg
m_s	1.00	Kg
m_w	1.00	Kg
k_s	400.00	Nm
k_w	5.00	Nm
c_s	7.00	Ns/m
c_w	7.00	Ns/m
ℓ	1.00	m
d	0.60	m
d_{Acmb}	0.50	m
	5	
M_θ	10	Nm
	20	
$I_{b,\text{cm}}$	0.1667	Kg/m^2

the contact force, as can be seen in these figures. A sudden change in velocity, when collision takes place, can be verified clearly in these figures.

5.2. Considering Different Values of M_θ

Table 2 shows numerical values considered in the numerical simulations for different values of M_θ.

6. Conclusions

To conclude, it is important to say that the time step used in the numerical integration and the choice of the integrator are very important aspects to be considered. New numerical

integrators can be tested in the course of this investigation and results compared to the ones presented here.

An important consideration not to be forgotten when dealing with problems presenting some sort of constraint is that more than one set of governing equations of motion must be integrated to cover all the system dynamics. The set of equations that governs the system dynamics when the constraint condition is active is different from the one that governs the unconstrained movement of the system. One of these sets is always generating the states for the other.

In this context, the determination of the velocities after contact (impact) is very important. The velocity expressions presented in (4.33) are the necessary corrections one must do when considering the fully plastic impact case. If this correction is not taken into consideration in the numerical integration of the governing equations, the system will gain energy after impact, which is not true.

It is important to realize also that the number of degrees of freedom involved changes from one set of equations to the other. The necessity for changing from one set of governing equations to another (according to the system's requirements of contact or noncontact conditions) represents a source of integration errors, since the integrator is faced with singularities.

The problem presented in this paper and the procedures developed for its analysis can be extended to many other systems and situations (including more complex ones). The theory presented here can be applied to problems in which robots have to follow some prescribed patterns or trajectories when in contact with the environment (like in painting activities, for instance, or the ROKVISS experiment at DLR).

The next steps are the development of the analytical expressions for the velocities after impact considering any value for the coefficient of restitution and the inclusion of friction forces between m_s and the left and right vertical guiding surfaces; and between the free end of the bar and m_w.

References

[1] F. Pfeiffer and C. Glocker, *Multibody Dynamics with Unilateral Contacts*, Wiley Series in Nonlinear Science, John Wiley & Sons, New York, NY, USA, 1996.

[2] C. Lánczos, *The Variational Principles of Mechanics*, Mathematical Expositions, no. 4, University of Toronto Press, Toronto, Canada, 4th edition, 1970.

[3] E. T. Whittaker, *A Treatise on the Analytical Dynamics of Particles and Rigid Bodies*, Cambridge University Press, Cambridge, UK, 1965.

[4] N. A. Fufaev and J. I. Neimark, *Dynamics of Nonholonomic Systems*, American Mathematical Society, 1972.

[5] A. Fenili, L. C. G. Souza, and B. Schäfer, "A mathematical model to investigate contact dynamics in constrained robots," in *Proceedings of the 6th International Symposium on Dynamic Problems of Mechanics (DINAME '05)*, D. A. Rade and V. Steffen Jr., Eds., Ouro Preto, Brazil, February-March 2005.

[6] B. Schäfer, B. Rebele, and A. Fenili, "Space robotics contact dynamics investigations and numerical simulations: ROKVISS," in *Proceedings of the 15th CISM-IFToMM Symposium on Robot Design, Dynamics and Control*, 2004.